

Diagnosis of precipitate formation in pulsed-laser deposition of $\text{YBa}_2\text{Cu}_3\text{O}_{7-\delta}$ by means of *in situ* laser-light scattering and *ex situ* atomic force microscopy

N. Kanda

Materials and Structures Laboratory, Tokyo Institute of Technology, Nagatsuta, Midori, Yokohama 226, Japan

M. Kawasaki*

Department of Innovative and Engineering Materials, Tokyo Institute of Technology, Nagatsuta, Midori, Yokohama 226, Japan

T. Kitajima

Materials and Structures Laboratory, Tokyo Institute of Technology, Nagatsuta, Midori, Yokohama 226, Japan

H. Koinuma*

Materials and Structures Laboratory, Tokyo Institute of Technology and CREST-Japan Science and Technology Corporation, Nagatsuta, Midori, Yokohama 226, Japan

(Received 24 March 1997)

We have developed a technique using laser-light scattering for monitoring and controlling precipitate formation during pulsed-laser deposition of $\text{YBa}_2\text{Cu}_3\text{O}_{7-\delta}$ (YBCO) films. By laser ablating a stoichiometric YBCO target under optimum conditions for preparing high-crystallinity YBCO films, it has been almost inevitable to have precipitates on the film surface. The dominant phases of the precipitates analyzed by μ -Auger mapping were Y-deficient compounds (CuO and BaCuO_2). The progress of precipitate formation at the very beginning of the film growth could be monitored *in situ* by measuring the intensity of the light scattered to a nonspecular direction after being impinged obliquely on the film surface. The increase of scattered light intensity was verified to result mainly from the increase of the precipitate size from the qualitative analysis of *ex situ* atomic force microscope images and Rayleigh scattering theory. We have proposed that the precipitates were segregated from the highly crystalline 123 phase and their formation proceeded in two steps, i.e., nucleation and growth. Then, we could expect the precipitate segregation could be reduced either by a two-step process with the aid of optical scattering data to readjust the averaged film stoichiometry or preventing the nucleation to reduce the segregated precipitates. By switching the target to an yttrium-rich (50%) pellet ($\text{Y}_{1.5}\text{Ba}_2\text{Cu}_3\text{O}_{7-\delta}$) after the deposition of 10-unit-cell-thick YBCO having precipitates, a decrease in the scattered light intensity was observed to be consistent with the reduction of precipitate. This is attributed to the compensation of the yttrium deficiency and conversion of the Y-deficient precipitates into the YBCO phase by the reaction with Y-rich ablated species. Thus the measurement of light scattering is shown to be a useful tool not only for analyzing the surface reactions, but also for suppressing precipitate formation. [S0163-1829(97)09137-6]

I. INTRODUCTION

Precipitate formation on $\text{YBa}_2\text{Cu}_3\text{O}_{7-\delta}$ (YBCO) thin films is one of the most serious problems preventing the fabrication of leakage-free Josephson tunnel junctions. Recently, we have elucidated that even a small deviation from stoichiometry ($\sim 1\%$ Y deficiency) could induce segregation of phases which consist of excess elements (predominantly CuO and BaCuO_2) on the films prepared by pulsed laser deposition (PLD), especially under the conditions optimized for getting high crystallinity and excellent superconducting properties.¹ For such multicomponent compounds, it is almost impossible to adjust the stoichiometry of the deposited elements exactly, unless self-organization controls the stoichiometry in a way similar to the vapor phase epitaxy of GaAs, where excess As can be removed due to the low sticking coefficient.²

In a molecular beam epitaxy (MBE) of such complex metal oxides as high- T_c superconductors, the film composition is determined by the supplied flux of constituting ele-

ments whose sticking coefficient is close to unity. The supplied flux of each element is individually controlled by using such flux-monitoring techniques as atomic absorption³ and crystal resonance detection. The stoichiometry is determined by the accuracy of the monitoring method, which is typically not better than 1%. For PLD, the fluctuations in laser fluence and target morphology could induce off-stoichiometry. Thus, if one wishes to eliminate the precipitate under the conditions which preserve high crystallinity of the films, one has to develop an *in situ* technique for monitoring the precipitate formation to bring the system to recrystallize the precipitates into the desired structure by adjusting the stoichiometry of the species supplied on the film surface.

Control of stoichiometry in this way may be done by monitoring the surface morphology on an atomic scale with reflection high-energy electron diffraction (RHEED). Characteristic spots in the RHEED pattern were observed for the segregation of Cu_2O during MBE growth of YBCO (Ref. 4) as well as for either Cu_2O or La_2O_3 during MBE of La_2CuO_4 depending on the net ratio of La/Cu in the flux.⁵ Naito and

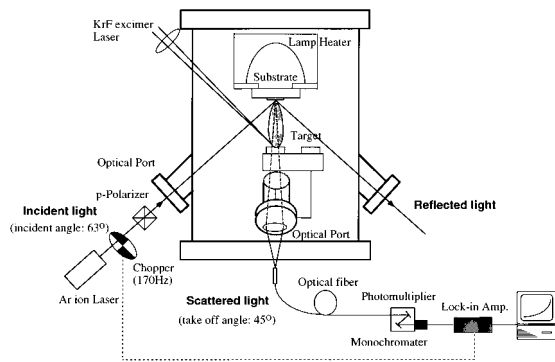


FIG. 1. Schematic illustration of pulsed laser deposition system equipped with *in situ* light scattering measurement system.

Sato have pointed out the possibility to feed back the RHEED results to readjust the stoichiometry of the flux ratio.⁵ However, there have been no reports of stoichiometry control under relatively high pressures where RHEED cannot be used. We have reported that such values as the thickness and optical constants of the films could be *in situ* measured during PLD of YBCO by monitoring the reflection intensity of *p*-polarized diode laser beam obliquely impinged on the film surface.⁶ When the film had high density of precipitates, we could detect it as a decrease of reflectance by scattering loss. In this study, we have detected the scattered light instead of the reflected light. Laser-light scattering was also reported to be useful for detecting Ga droplets during GaAs growth under As-deficient conditions.⁷ This method is applicable for detecting objects even smaller than the wavelength of the light. For instance, Epler and Schweizer observed intensity oscillation of scattered light with a period of monolayer growth during GaAs homoepitaxial growth, presumably due to the light scattering at the unit-cell high steps.⁸

In this work, we used laser-light scattering for monitoring precipitate formation on laser ablated YBCO films under a relatively high oxygen pressure. The increase of light scattering during the film growth was shown to be due to the increase of the precipitate size from the detailed comparison with *ex situ* atomic force microscope (AFM) results. A preliminary result is given for applying this technique to the recrystallization of precipitates (CuO , BaCuO_2) into desired phase (YBCO) by compensating the deficient element (Y).

II. EXPERIMENT

YBCO films were prepared by pulsed KrF excimer laser (Lambda Physik, LPX 100, 1 J/cm^2 , 1 Hz deposition from a stoichiometric target. The films were deposited at a substrate temperature of $750 \text{ }^\circ\text{C}$ and an oxygen pressure of 600 mTorr. A schematic illustration of the *in situ* laser-light scattering measurement system is shown in Fig. 1. An Ar ion laser beam (NEC, GL S3260J, 488 nm, 100 mW) was *p* polarized, modulated at 170 Hz by a chopper, and impinged on the surface at an incident angle of 63° . Shorter-wavelength (λ) laser light was preferred because the Rayleigh scattering by a small object is enhanced as a function of λ^{-4} . The reflected light was measured to monitor the thickness and optical constants of the growing films as already reported in Ref. 6. A part of the scattered light was introduced through a quartz

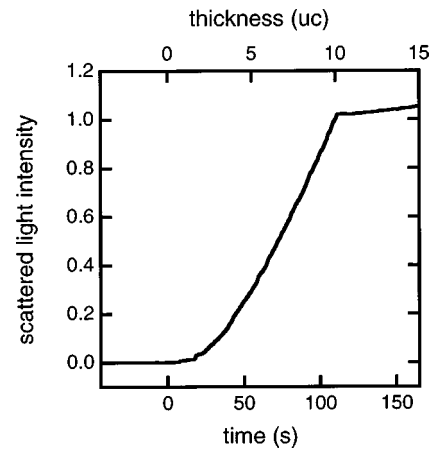


FIG. 2. Variation of scattered light intensity during YBCO initial growth up to 10 unit cells thick.

window to the optical fiber connected with the monochromator and lock-in amplifier. The scattering direction was 45° from normal, and its projection on the film surface was perpendicular to the incident-reflected beam plane. In this geometry, the scattering angle was 79° and the scattering vector (K) was $13.8 \mu\text{m}^{-1}$ (correlation length $\sim 0.46 \mu\text{m}$). Nb (1 wt %) doped $\text{SrTiO}_3(100)$ substrates were used because of its large absorption coefficient which prevented undesired light scattering at the back side and bulk crystal defects of the substrate.

In order to examine the relationship between the scattered light intensity and the film surface morphology, we quenched the film by turning the heater off and analyzed the surface morphology by atomic force microscopy (AFM, SEIKO SPI 3700) with a standard Si_3N_4 tip (20-nm-diam equivalent). The AFM image is a convolution of the surface morphology and tip geometry, but the size of precipitates discussed in this paper is far larger than the tip radius and therefore the error of the precipitate volume estimated from AFM image is negligibly small.

III. RESULTS AND DISCUSSION

A. Precipitate formation during initial growth

The pulsed laser deposition at a rate of 0.11 nm/pulse from a stoichiometric $\text{YBa}_2\text{Cu}_3\text{O}_{7-\delta}$ target gave *c*-axis-oriented epitaxial films with small precipitates on the surface. The films exhibited high crystallinity and excellent superconducting properties.⁹ In our previous paper, we concluded that the precipitates with a quite high density ($>10^7 \text{ cm}^{-2}$) had already nucleated at the initial stage (thickness $<50 \text{ nm}$) of the film growth and subsequent deposition made precipitates larger keeping the same density.¹ Here we report a detailed analysis by *in situ* light scattering and *ex situ* AFM for the very beginning of the YBCO growth on the commercial SrTiO_3 substrate.¹⁰

Figure 2 shows the scattered light intensity observed during the growth of the initial 10 unit-cell (uc) layers of $\text{YBa}_2\text{Cu}_3\text{O}_{7-\delta}$ film. The scattered light intensity monotonously increased just after the deposition started. This result suggests that the precipitates were formed from the very beginning of the film growth. To confirm this behavior, *ex situ* AFM analysis was performed at various stages by quenching

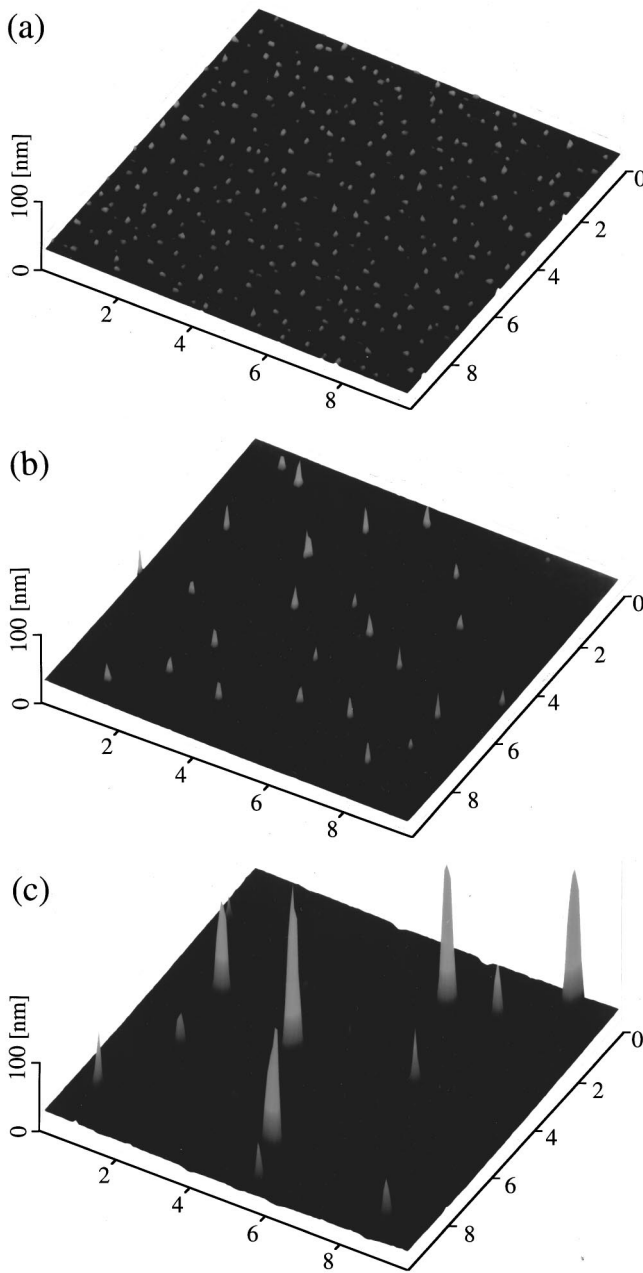


FIG. 3. AFM images of YBCO films at various thicknesses. (a) 1 uc, (b) 3 uc, and (c) 10 uc. The scan area was $10 \mu\text{m} \times 10 \mu\text{m}$. Film thickness dependences of quantitative data extracted from AFM images.

the films. As shown in Fig. 3, the precipitates had already appeared on 1 uc (unit cell) YBCO. The typical height and lateral size of the precipitates were 10 and 200 nm, respectively, far smaller than the wavelength. Smith observed the increase of scattered light intensity from Ar ion laser beam due to the pits formed on a GaAs wafer during oxide desorption by heating the substrate up to 630°C .¹¹ The pits were 5–10 nm in depth and 20–200 nm in lateral size, which are comparable to the sizes of the precipitates on 1 uc YBCO. Therefore, the initial increase of light scattering can be reasonably counted as the precipitate formation on YBCO film. AFM measurements at the subsequent stages revealed that the precipitates became larger, but their density decreased as the film thickness increased.

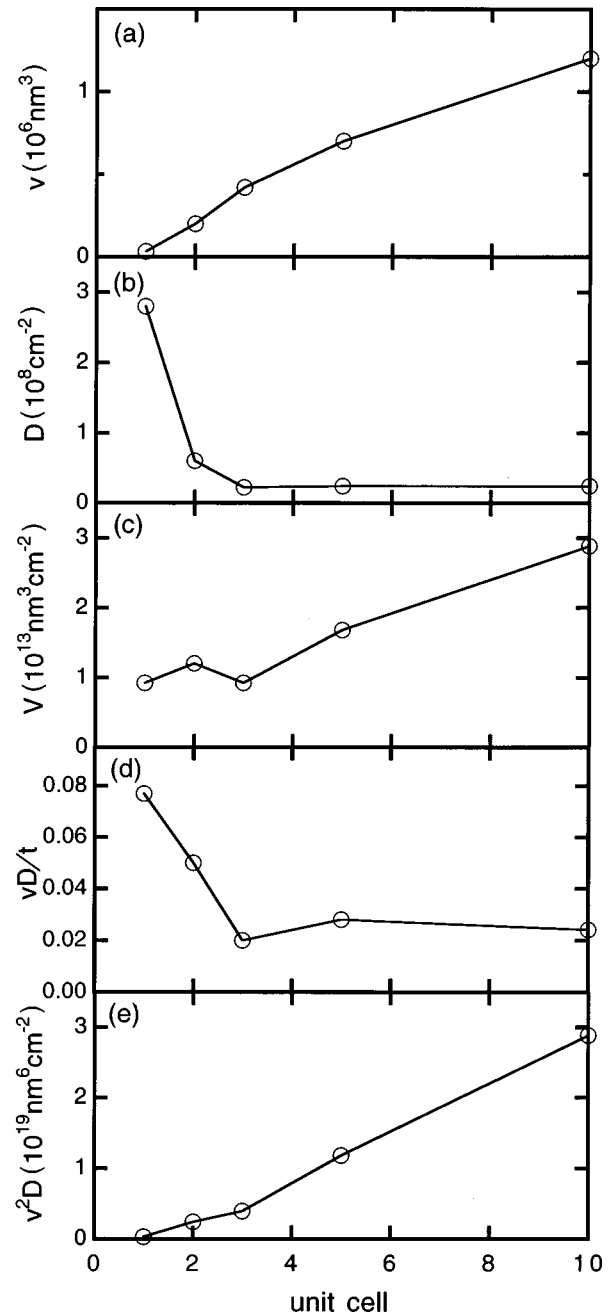


FIG. 4. (a) Average volume of a precipitate (v). (b) Precipitate density (D). (c) Total volume ($V=vD$). (d) Volume fraction (vD/t) of the precipitate to the nominal film volume. (e) A parameter, v^2D , which should be proportional to the scattered light intensity under Rayleigh scattering approximation.

The quantitative analyses of AFM images gave further important information about the nucleation and growth of the precipitates. As the shape of the precipitates appeared to be a cone in the AFM images, we assumed the volume (v) of a precipitate to be $S \times h/3$, where S is the area of precipitate in an AFM image and h is the height of the precipitate. The mean value of the volume for a precipitate is plotted in Fig. 4(a) as a function of the film thickness. The density (D) of the precipitate [Fig. 4(b)] was evaluated from AFM images ($10 \mu\text{m} \times 10 \mu\text{m}$). The total volume of the precipitate per unit area (cm^2) and the volume fraction were thus evaluated as Dv and Dv/t , respectively, where t is the nominal thickness

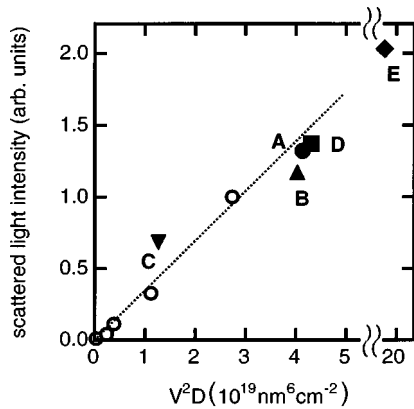


FIG. 5. Relationship between scattered light intensity and v^2D taken from Fig. 4 are plotted by \circ . This linear relationship indicates the scattered light is due to the precipitates existing on the film surface during the deposition. The points shown by \bullet , \blacktriangle , \blacksquare , \blacktriangledown , and \blacklozenge are the data for the films A, B, C, D, and E in Fig. 7, respectively. The dotted line is a guide to eye.

of the film. As shown in Fig. 4(a), mean value of the precipitate volume increased monotonously. The density of precipitate was quite high ($3 \times 10^8 \text{ cm}^{-2}$) at 1 uc, but rapidly decreased to a steady value of $2 \times 10^7 \text{ cm}^{-2}$, which coincides with the value evaluated by scanning electron microscopy (SEM) images for hundreds nm thick films. Therefore, the nucleation of precipitates took place when the very first monolayer of YBCO was deposited, followed by the growth.

In order to correlate the scattering intensity with the above quantitative data deduced from AFM pictures, we consider the scattered light intensity based on Rayleigh approximation. When the object size is much smaller than the wavelength, the light scattered by the object can be described by the Rayleigh approximation $I = E^2$ where E is the electric field of scattered light and is proportional to the dipole moment of the object. When the object is smaller than the penetration depth of the light, the total dipole moment of the object is proportional to its volume. Therefore, the scattered light intensity from a particle is proportional to v^2 .¹² Thus the total scattered light intensity from particles with a density of D is proportional to v^2D , which is plotted in Fig. 4(e) as a function of film thickness to show the monotonous increase. The open circles in Fig. 5 are plotted to show the relationship between v^2D and scattered light intensity (I) shown in Fig. 1. This linear relationship indicates that the light scattering during the initial growth of YBCO was indeed caused by the presence of precipitates. Thus we conclude that the variation of total volume of the precipitates could be evaluated *in situ* by monitoring the scattered light intensity.

Now we concentrate on the mechanism of precipitate formation. As shown in Fig. 4(d), the volume fraction of precipitate at 1 uc is as high as 8%. For identifying the phase of the precipitates at the very initial stage, a RHEED pattern was taken at an incident angle as small as possible. Together with the streaks due to the two-dimensional perovskite surface, we could detect diffused spots due to the transmission of electron beam through the precipitates. By comparing the pattern with those for rather rough Cu_2O , CuO , and BaCuO_2 films, we concluded that the majority of the precipitates was

CuO . The 8% precipitate volume fraction corresponds to one atomic layer of CuO_x among six atomic layers of $\text{YBa}_2\text{Cu}_3\text{O}_{7-\delta}$. Therefore, the matrix film covering the SrTiO_3 substrate is presumed not to be $\text{YBa}_2\text{Cu}_3\text{O}_{7-\delta}$, but $\text{YBa}_2\text{Cu}_2\text{O}_x$. Kawai *et al.*¹³ and we¹⁴ specified that the surface of SrTiO_3 substrate was predominately terminated by a TiO_2 atomic layer, which is a B -site layer in perovskite ABO_3 . Assuming that the A -site layer (Y or Ba) comes preferentially on top of the TiO_2 layer with preserving the YBCO lattice structure,¹⁵ the topmost layer would be a B -site cation (either CuO chain or CuO_2) layer after the deposition of 1-uc-thick YBCO. However, the topmost atomic layer of the films in this study must be an A -site layer since one atomic layer of CuO segregates as precipitates. Similar conversion of topmost layer from the B -site layer to the A -site layer during epitaxy of perovskite compounds was also observed by us in heteroepitaxy of SrCuO_2 (Ref. 16) on SrTiO_3 and homoepitaxy of SrTiO_3 .¹⁷

As the film became thicker, the volume fraction of the precipitate gradually decreased to reach a constant value of 2.5% at 5 uc growth and more. This result indicates that the average off-stoichiometry of species supplied under these conditions was a few percent. As a reason why the precipitate density decreased, we propose a scheme as follows. The distance between two adjacent precipitates can be regarded as a diffusion length of the off-stoichiometric species.¹ If we assume the diffusion length on SrTiO_3 is short but that on YBCO is long, we can explain the decrease of precipitate in the following way. First, CuO precipitates nucleate densely. Some of them serve as nucleation sites for forming larger CuO and BaCuO_2 precipitates which were observed on thicker films. The other majority just disappears by the desorption of Cu -related species from preexisting CuO precipitates to migrate again on the film surface and to be incorporated in the growing precipitates. These phenomena can be well understood if the critical size of nuclei is small on SrTiO_3 and becomes large on YBCO because of the difference of free energy at the interface.

B. Precipitate elimination by supplying Y-rich species

From the results and discussion presented above, it is clear that the segregation of precipitates started at the first monolayer growth of YBCO. The subsequent deposition induced the growth of precipitates. Let us discuss here how the optical scattering can be used to eliminate the precipitates. Precipitates on 10 uc YBCO films were identified by μ -Auger electron spectroscopy to be mainly CuO and BaCuO_2 in a similar way to that in Ref. 1. Therefore, the average composition of the deposited elements should be in the Y-deficient region hatched in the $\text{YO}_{1.5}$ - BaO - CuO pseudoternary equilibrium phase diagram¹⁸ (Fig. 6). If one supplies Y-rich species after the growth of YBCO, one will be able to move the total composition of the system close to 123 along the line between $\text{YO}_{1.5}$ - $\text{Ba}_2\text{Cu}_3\text{O}_x$ and the average composition of precipitates. To supply extra Y atoms, we used a $\text{Y}_{1.5}\text{Ba}_2\text{Cu}_3\text{O}_{7-\delta}$ ($\text{Y}_{1.5}\text{BCO}$) target and ablated it under the same conditions as those used for the ablation of YBCO target. We did not choose Y_2O_3 or Y_2BaCuO_5 targets because they can stably coexist with YBCO and these compounds were frequently observed as impurity phases in

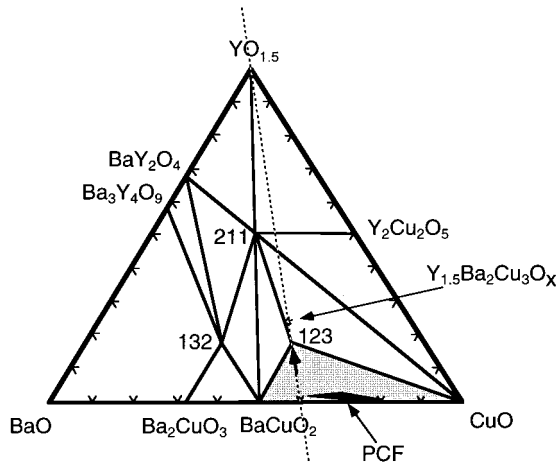


FIG. 6. Pseudoternary phase diagram of $YO_{1.5}$ -BaO-CuO at 850 °C and 1 atm oxygen pressure (Ref. 18). The composition of $Y_{1.5}Ba_2Cu_3O_{7-\delta}$ is marked by an asterisk. The hatched area shows the region where YBCO can coexist with $BaCuO_2$ and CuO. The primary crystallization field is also shown (Ref. 23) by the solid triangle.

YBCO films with Y-rich average composition.¹⁹ When we deposited 300-nm-thick films from the $Y_{1.5}BCO$ target, the films were turned out to be *c*-axis-oriented YBCO having poor crystallinity and high density ($2 \times 10^7 \text{ cm}^{-2}$) of Y_2O_3 and Y_2BaCuO_5 precipitates. The overall composition of the films was the same as that of the target according to the results obtained by the inductively coupled plasma (ICP) analysis. The deposition rate of the films was the same, 0.11 nm/pulse, for the both targets.

First, 10 uc YBCO film was deposited from the stoichiometric target, and then 0.5 uc $Y_{1.5}BCO$ was deposited on the YBCO film. The volume fraction of precipitates on 10 uc YBCO films was about 2.5%. In order to compensate the Y deficiency in these precipitates, the deposition of 0.5 uc $Y_{1.5}BCO$ should be required, if we assume Ba/Cu ratio averaged over the precipitates is 2/3.

Figure 7(a) shows the variation of scattered light intensity observed during and after the depositions of 0.5 uc $Y_{1.5}BCO$ on top of the 10 uc YBCO. For the comparison, we also carried out the deposition of 0.5 uc YBCO on top of the 10 uc YBCO under otherwise the same conditions [Fig. 7(b)]. Curve (a) continued to increase slightly after the deposition of the initial YBCO layer but started to decrease just after 0.5 uc $Y_{1.5}BCO$ was deposited. On the other hand, when 0.5 uc YBCO was deposited, the scattered light intensity continued to increase [curve (b)]. To correlate the scattered light intensity with surface morphology, we carried out again the AFM observation for the films quenched at stages denoted by A, B, C, D, and E in Fig. 7. Figures 8(a) and 8(b) show AFM images of the films kept at the deposition temperature for 45 min after the deposition of 0.5 uc $Y_{1.5}BCO$ (D) and YBCO (E), respectively. If we compare them with the AFM image for the 10 uc YBCO film shown in Fig. 3(c), the changes of the surface morphology are clear. The size of precipitates decreased drastically by depositing 0.5 uc $Y_{1.5}BCO$, as shown in Fig. 8(a). The volume fraction of the precipitates decreased from 2.5% to 1.0%. On the other hand, the size of

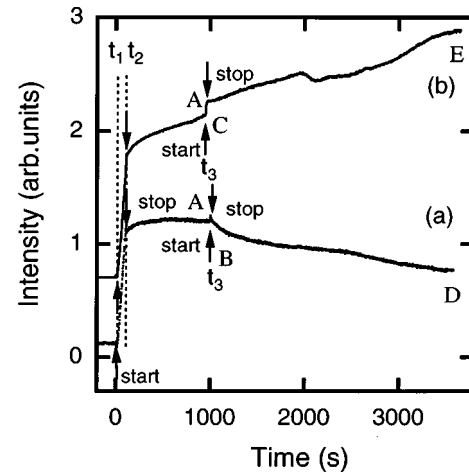


FIG. 7. Variation of scattered light intensity observed during the two-step deposition process. (a) 0.5-uc-thick Y-rich YBCO ($Y_{1.5}Ba_2Cu_3O_x$) was deposited on 12-nm-thick YBCO film. (b) Second deposition was also carried out by using stoichiometric YBCO target.

precipitates increased after the deposition of 0.5 uc YBCO, as shown in Fig. 8(b). By depositing $Y_{1.5}BCO$, the surface morphology of the matrix film between the precipitates was kept flat, i.e., similar to that shown in Fig. 2 of Ref. 20,

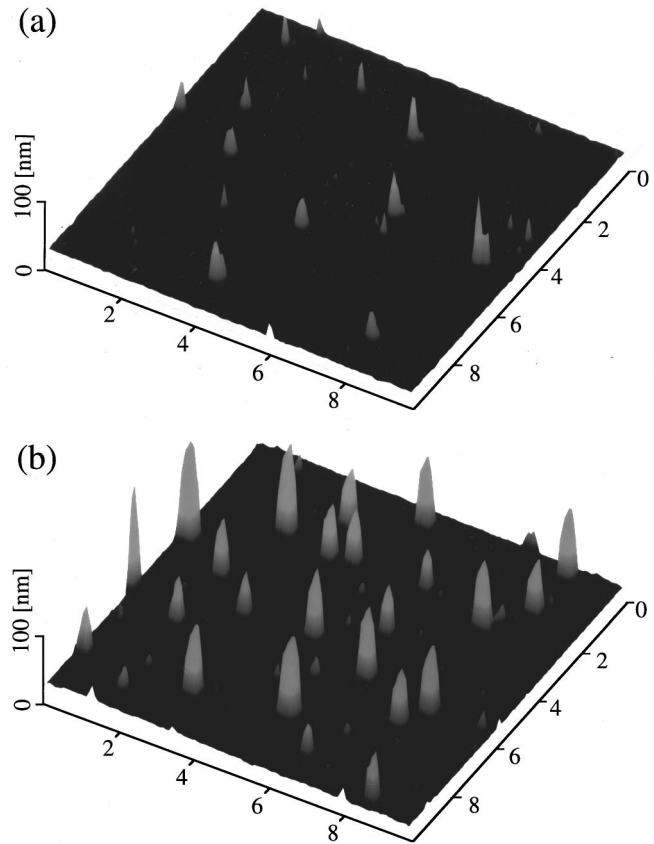


FIG. 8. AFM images of the YBCO film surfaces 45 min after the deposition of 0.5-uc-thick $Y_{1.5}Ba_2Cu_3O_{7-\delta}$ (a) and $YBa_2Cu_3O_{7-\delta}$ (b) on 10 uc YBCO films. The scan area was $10 \mu\text{m} \times 10 \mu\text{m}$. By supplying Y-rich species, the volumes of the precipitates were greatly reduced.

where clear step (1.2 nm) and terrace structure was seen. Therefore, we conclude that the two-step growth can indeed control the volume of the precipitate. The AFM images of the films quenched at the stages *B* and *C* (immediately after the deposition of 0.5 μm films) were very little different from the image of the film quenched at the stage *A*, being consistent with little changes in the scattering intensity. The scattered light intensity and v^2D for the films at the stages from *A* to *E* are also plotted in Fig. 5. The points for stages *A*, *B*, *C*, and *D* are on the linear line drawn in the Rayleigh approximation, whereas the point *E* is deviated from the line (too small scattered light intensity). This can be explained if we assume that the precipitates at stage *E* were too large to be treated by the Rayleigh approximation. The scattering occurred only by the dipole moment near the surface to result in the lower scattered light intensity because the incident light cannot penetrate in the bulk of precipitate. From the changes in scattered light intensity after the deposition of 0.5 μm films (*C* to *E* and *B* to *D*), the reaction between the precipitates and the supplied species should proceed very slowly.

The real time observation of the surface reaction of YBCO growth have been scarcely made except for such processes under low oxygen pressures as MBE. The diffusion times of activated adatoms in low pressure processes were fast, in the order of a few tens of seconds, as estimated from the recovery time of RHEED intensity.²¹ The reaction between the precipitates and the ablated species in this case of PLD was so slow that it took 30 min or more. This difference in reaction time scale indicates that the surface reaction in PLD is different from that in MBE. In PLD, most of ablated species should be oxidized in vapor phase before they arrive at the film growing surface,²² whereas the unoxidized species could arrive at the surface in MBE. The surface diffusibility of the oxidized species is presumed to be lower than that of unoxidized species.

It is important to control precisely the composition of YBCO films to achieve 123 stoichiometry and prevent the precipitate formation caused by off-stoichiometry. However, our previous research showed that highly crystalline YBCO films could be fabricated only in the Y-deficient region in the phase diagram, to make the formation of Y-deficient precipitates almost inevitable.¹ This tendency can be understood by considering the location of the primary crystallization field (PCF) where crystallization directly from liquid is possible in the phase diagram. The PCF of YBCO is known to be in the Y-deficient area²³ as shown in Fig. 6. This is why the Czochralski growth of YBCO single crystal is carried out from a BaO-CuO melts as self-solvents.²⁴ To fabricate

highly crystalline YBCO films, it is also important to crystallize the film from Y-deficient species migrating on the film surface. This is why we always observed BaCuO₂ and CuO precipitates on highly crystalline YBCO films. If one wishes to have highly crystalline films without precipitates, the two-step growth proposed in this paper should be effective. As the first step, Y-deficient species are supplied to grow highly crystalline YBCO films from PCF and then Y-rich target is used to compensate the off-stoichiometry. By repeating these alternating depositions with the detection of precipitates by the optical scattering, highly crystalline YBCO films with small amount of precipitates should be formed.²⁵ In order to grow films of such binary compounds as La₂CuO₄, an adjustment of net composition can be achieved by switching two kinds of targets. In contrast, YBCO is a line phase compound having ternary elements. There has to be two degrees of freedom in order to precisely adjust the net composition. Since the optical scattering cannot detect the net ratio of Ba/Cu for the precipitates, supplying Y-rich species only at the same Ba/Cu ratio cannot eliminate completely the precipitates. Even the compound is ternary, this method can be applicable to La_{2-x}Sr_xCuO₄, for example. If the (La+Sr)/Cu ratio is to be adjusted, the precipitate will be eliminated because La and Sr ions can be solid soluted in a wide range of composition.

IV. CONCLUSIONS

We have established a diagnostic method to monitor the precipitate formation by laser-light scattering during the film growth of YBCO. This method can be used under such high-pressure processes as PLD and metal-organic chemical-vapor deposition (MOCVD) without any damage on the surface. The scattered light intensity was shown to have good correlation with the total volume of the precipitates. By this diagnosis together with *ex situ* AFM results, CuO precipitates are shown to nucleate at the very beginning of YBCO growth and to serve as nucleation site for precipitating BaCuO₂ and CuO. By supplying Y-rich species on the YBCO film, the precipitates can be recrystallized into YBCO to reduce the total volume. The concept of this two-step growth for eliminating the precipitates was discussed on the basis of thermodynamics and kinetics.

ACKNOWLEDGMENT

This work was partly supported by JSPS Research for the Future Program in the area of Atomic-Scale Surface and Interface Dynamics (RFTF96P00205).

*Authors to whom correspondence should be addressed.

Electronic addresses: kawasaki@oxide.rlem.titech.ac.jp, koinuma@oxide.rlem.titech.ac.jp

¹J. P. Gong, M. Kawasaki, K. Fujito, R. Tsuchiya, M. Yoshimoto, and H. Koinuma, Phys. Rev. B **50**, 3280 (1994).

²M. Kawasaki, N. Kanda, R. Tsuchiya, N. Nakano, A. Ohtomo, K. Takahashi, H. Kubota, T. Shiraiishi, and H. Koinuma, Adv. Supercond. **8**, 1023 (1996).

³I. Bozovic and J. N. Eckstein, MRS Bull. **20**, 32 (1995).

⁴J.-P. Locquet, A. Catana, E. Machler, C. Gerber, and J. G. Bed-

norz, Appl. Phys. Lett. **64**, 372 (1994).

⁵M. Naito and H. Sato, Appl. Phys. Lett. **67**, 2557 (1995).

⁶N. Kanda, M. Kawasaki, K. Nakano, T. Shiraiishi, A. Takano, and H. Koinuma, Jpn. J. Appl. Phys., Part 1 **36**, 2103 (1997).

⁷J. M. Olson and A. Kibbler, J. Cryst. Growth **77**, 182 (1986).

⁸J. E. Epler and H. P. Schweizer, Appl. Phys. Lett. **63**, 1228 (1993).

⁹M. Kawasaki, J. P. Gong, M. Nantoh, T. Hasegawa, K. Kitazawa, M. Kumagai, K. Horiguchi, M. Yoshimoto, and H. Koinuma, Jpn. J. Appl. Phys., Part 1 **23**, 1612 (1993).

- ¹⁰Even if we used atomically flat SrTiO₃ terminated with TiO₂ plane (Ref. 17), qualitatively similar results were obtained. Details will be reported elsewhere.
- ¹¹G. W. Smith, A. J. Pidduck, C. R. Whitehouse, J. L. Glasper, A. M. Keir, and C. Pickering, *Appl. Phys. Lett.* **59**, 3282 (1991).
- ¹²A. M. Bonnot, B. S. Mathis, and S. Moulin, *Appl. Phys. Lett.* **63**, 1754 (1993).
- ¹³M. Kawai, Z.-Y. Liu, T. Hanada, M. Katayama, M. Aono, and C. F. McConville, *Appl. Surf. Sci.* **82-83**, 487 (1994).
- ¹⁴M. Yoshimoto, T. Maeda, K. Shimozone, H. Koinuma, M. Shiohara, O. Ishiyama, and F. Ohtani, *Appl. Phys. Lett.* **61**, 2659 (1992).
- ¹⁵J. P. Wen, C. Traeholt, and H. W. Zandbergen, *Physica C* **205**, 354 (1993).
- ¹⁶S. Gonda, H. Nagata, M. Kawasaki, M. Yoshimoto, and H. Koinuma, *Physica C* **216**, 272 (1993).
- ¹⁷M. Kawasaki, K. Takahashi, T. Maeda, R. Tsuchya, M. Shiohara, O. Ishiyama, T. Yonezawa, M. Yoshimoto, and H. Koinuma, *Science* **266**, 1540 (1994).
- ¹⁸B. T. Ahn, V. Y. Lee, and B. Beyers, *Physica C* **167**, 529 (1990).
- ¹⁹O. Eibl and B. Roas, *J. Mater. Res.* **5**, 2620 (1990).
- ²⁰M. Kawasaki and M. Nantoh, *MRS Bull.* **19**, 33 (1994).
- ²¹T. Frey, C. C. Chi, C. C. Tsuei, T. Shaw, and F. Bozso, *Phys. Rev. B* **49**, 3483 (1994).
- ²²A. Gupta, *J. Appl. Phys.* **73**, 7877 (1993).
- ²³H. J. Scheel and F. Licci, *Thermochim. Acta* **174**, 115 (1991).
- ²⁴S. Takekawa and N. Iyi, *Jpn. J. Appl. Phys., Part 1* **26**, L851 (1987).
- ²⁵The electrical properties of the films prepared in this study were not measured. The thick films (>20 nm), having high crystallinity and precipitates (BaCuO₂ and CuO), always showed high T_c and J_c . Therefore, we expect excellent electrical properties for the films prepared under the thermodynamic control in this study, unless the film is so thin that the stress caused by lattice mismatch reduces T_c for the films thinner than 5 nm.